

Memetic Algorithms for Ligand Expulsion from Protein Cavities

J. Rydzewski^{1, a)} and W. Nowak¹

Institute of Physics, Faculty of Physics, Astronomy and Informatics, Nicolaus Copernicus University, Grudziadzka 5, 87-100 Torun, Poland

This is the updated version of work published previously in *J. Chem. Phys.* **143**, 124101 (2016).¹

Ligand diffusion through proteins is a fundamental process governing biological signaling and enzymatic catalysis. The complex topology of protein tunnels results in difficulties with computing ligand escape pathways by standard molecular dynamics (MD) simulations. Here, two novel methods for searching of ligand exit pathways and cavity exploration are proposed: memory random acceleration MD (mRAMD), and memetic algorithms (MA). In mRAMD, finding exit pathways is based on a non-Markovian biasing that is introduced to optimize the unbinding force. In MA, hybrid learning protocols are exploited to predict optimal ligand exit paths. The methods are tested on three proteins with increasing complexity of tunnels: M2 muscarinic receptor, nitrile hydratase, and cytochrome P450cam. In these cases, the proposed methods outperform standard techniques that are used currently to find ligand egress pathways. The proposed approach is general and appropriate for accelerated transport of an object through a network of protein tunnels.

I. INTRODUCTION

Ligand recognition is one of the most critical steps in biological signaling.² To pass a signal, a ligand usually binds to a specific receptor site which may be exposed on the receptor surface or buried within the receptor matrix. Ligand residence time is of crucial importance in regulatory processes.³ Entrance, binding and egress processes involve complex migration through the protein tunnels or ligand accessible cavities. Properties of these pathways determine rate of signaling. Uncovering the distributions of transport routes is important not only in understanding mechanisms of signal transduction, but also in enzymatic catalysis, molecular diseases, and drug design.⁴ Ligand dissociation may be studied computationally, but classical molecular dynamics (MD) suffers from the low probability of crossing energy barriers which kinetically entrap ligands in the protein matrix. To facilitate the crossing, and in turn, to increase rare conformational event probability, numerous enhanced MD methods have been developed so far, i.e., locally enhanced sampling (LES),^{5,6} targeted MD,⁷ steered MD (SMD),⁸ and supervised MD.⁹ For a review of enhanced MD methods see, for example, Ref. 10.

The techniques proposed here, mRAMD and MA, may be considered as an extension of SMD, with the time-dependent direction of the unbinding force. It is worth to mention that SMD in its original form is limited in sampling optimal ligand egress paths, because the unbinding force given by:

$$\mathbf{F} = -\frac{k}{2}\nabla_{\mathbf{r}}[vt - (\mathbf{r} - \mathbf{r}_0) \cdot \mathbf{n}]^2, \quad (1)$$

where k is a force constant, v is the constant unbinding velocity, \mathbf{r} and \mathbf{r}_0 are the current and the initial positions of a pulled atom, and \mathbf{n} is the unbinding direction; is kept constant during the simulation, so the sampled path is limited to a straight line. Also, the unbinding direction must be assumed a priori which is a severe drawback of SMD for protein tunnels that are nonlinear.

A solution for this problem was found by Lüdemann et al.¹¹ who introduced a method called random acceleration MD (RAMD), in which the unbinding direction is modified when the traveling ligand meets any steric obstacle.^{12,13} This method made the enforced egress of camphor from cytochrome P450cam possible with no prior knowledge of

^{a)}Email: jr@fizyka.umk.pl

exit tunnels.¹¹ Despite its popularity,^{14–16} RAMD has one drawback: a trade-off between artificial perturbation of the protein structure caused by the enforced ligand unbinding, and the low probability of sampling ligand unbinding events. In other words, many long trajectories have to be computed to get a reasonable statistics.^{11,17}

Here, two new methods for studying ligand transport through complex protein channels and tunnels are introduced: mRAMD and MA. Both find plausible unbinding paths from buried protein binding sites in the following test systems: M2 muscarinic receptor (M2), nitrile hydratase (NHase), and cytochrome P450cam (P450cam). The last system, P450cam, was studied in the original RAMD work¹¹ (Fig. 1).

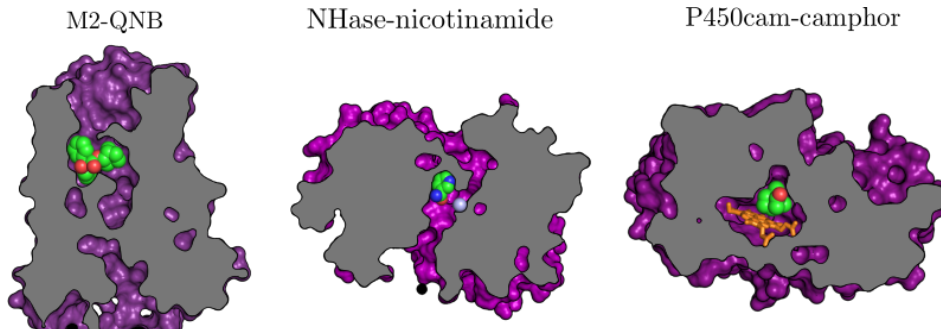


FIG. 1. Structures of the ligand-protein complexes studied in this article shown in increasing complexity of protein tunnels: M2-QNB, NHase-nicotinamide with cobalt (light blue) in the catalytic center of NHase, P450cam-camphor with heme shown (orange).

II. METHODS

A. Non-Markovian Variant of Random Acceleration MD

We start by introducing RAMD which is an extension of SMD that speeds up dissociation kinetics by few orders of magnitude, and allows to find various probable dissociation routes. Also no prior knowledge of an exit tunnel or channel is required. The RAMD protocol is the following:

1. The direction $\hat{\mathbf{r}}$ of the unbinding force acting on the center of mass of the ligand is assigned randomly, $\mathbf{f} = f\hat{\mathbf{r}}$, where f is a constant magnitude of the unbinding force.
2. The unbinding force is maintained for a predetermined number of simulation steps, m . The ligand is expected to move with a velocity exceeding the threshold velocity given by $v_t = r_t/m\Delta t$, where Δt is the time step and r_t is a specified minimum distance that the ligand passes before the unbinding direction changes. If this condition is not fulfilled, the unbinding direction is reassigned randomly.

Finding optimal values for all parameters in RAMD (r_t , f , m) for a ligand-protein complex is far from trivial. Vashisth and Abrams¹⁷ considered it to be a drawback of RAMD as the adopted force constant f should not be too high. This resulted in the percentage of successful dissociation events at about 19%-41%.¹⁷

We introduced modifications to the standard RAMD method. First, we added an additional heuristic constraint to decrease a high number of unsuccessful ligand unbinding trajectories from a receptor:

3. Next random unbinding direction is chosen if the distance traveled by the ligand during the current i th time interval $d(m\Delta t_i)$ of the simulation is smaller than the distance traveled in the previous interval $d(m\Delta t_{i-1})$. This usually happens when some steric obstacle emerges along the sampled unbinding route.

Second, we introduced a variant of RAMD with a non-Markovian dependency added (mRAMD). It was developed for finding the most probable egress pathways. The dependence on the previous simulated unbinding trajectories was

added to mRAMD as an additional positive reinforcement. This process, inspired by swarm optimization methods,¹⁸ leads to the initial random probing of the protein tunnels, but gradually while more trajectories are sampled, the ligand experiences not only the stochastic force in a random direction $f_0\hat{r}$, but also the force directed to dense regions of conformational space sampled by the previous trajectories $f_1\hat{k}$, i.e., $\mathbf{f} = f_0\hat{r} + f_1\hat{k}$.

The initial distribution of the ligand conformations in the protein tunnel is an important factor. A reasonably good guess can be obtained by running an exploratory LES⁵ simulation, or by simply collecting the previous conformations gradually from mRAMD simulations. Clearly, f_0 should be larger than f_1 , otherwise the resulting unbinding pathways would be constraint to the initial distribution of conformations, and their diversity would be limited.

During mRAMD simulations some paths may exhibit steric clashes and kinetic traps. To eliminate these problem we applied the following scheme to the positive reinforcement protocol in mRAMD:

1. To eliminate rarely visited paths, the reinforcement continuously decreases during the simulation according to $\rho_i = \rho_i(1 - q)$, where ρ_i is the density of the i th trajectory and q is a damping factor (set to 0.01).
2. Density of previous conformations is averaged. The Shepard approximation algorithm¹⁹ is used with KD-trees for finding nearest neighbors. This reduces the complexity of the Shepard method to $O(N \log N)$, where N is the number of interpolated neighbors.²⁰ We used the Liszka kernel²¹ (for details see Supporting Material).

B. Finding Unbinding Pathways with Non-Convex Optimization

Finding and exploring ligand unbinding pathways from proteins may be formulated in terms of an optimization problem. Solving such a problem is then equivalent to finding an extreme of a postulated multivariate scoring function. Here, out of many scoring-based metaheuristics suitable for such studies we used memetic algorithms (MAs) which are a good choice for non-convex scoring functions.^{22,23} MAs involve an iterative process of learning (i.e., adapting to the scoring function). Ligand conformations were represented by their center of mass positions within a predefined sampling radius, r_s , centered at the ligand.

The optimization scheme in MAs is the following:

1. Initially, the ligand conformations are chosen by sampling center of mass positions inside the sampling radius, r_s , centered at the current ligand conformation whose dynamics is given by the MD simulation.
2. The score $f^{(i)}$ of the i th conformation is calculated based on effective interaction energy between the corresponding ligand and the protein. In our implementation of MAs, we considered effective interaction energy consisting of four terms:

$$\begin{aligned}
 f^{(i)} = & \alpha_v \sum_{k<l} \left(\frac{A_{kl}}{r_{kl}^{12}} - \frac{B_{kl}}{r_{kl}^6} \right) \\
 & + \alpha_h \sum_{k<l} \left(\frac{C_{kl}}{r_{kl}^{12}} - \frac{D_{kl}}{r_{kl}^{10}} \right) \\
 & + \alpha_e \sum_{k<l} \frac{q_k q_l}{\epsilon(r_{kl}) r_{kl}} \\
 & + \alpha_s \sum_{k<l} (S_k V_l + S_l V_k) \exp(-r_{kl}^2/2\sigma^2),
 \end{aligned} \tag{2}$$

where the $\alpha_{(\cdot)}$ coefficients on the right-hand side are empirically determined using linear regression from a set of ligand-protein complexes.^{24,25} The summations are over ligand indices k and protein indices l . The first term is the Lennard-Jones 12-6 potential. The second term is hydrogen bond energy modeled by the Lennard-Jones 12-10 potential. A , B , C , and D are matrices calculated to mimic the depth of the Lennard-Jones potential well and equilibrium bond distances for homogeneous pairs of atoms. The third term describes the Coulombic

potential, where q is the charge of a given atom. The distance-dependent dielectric variable is modeled by a sigmoid:

$$\epsilon(r) = a + \frac{b}{1 + k \exp(-\lambda br)} \quad (3)$$

where $b = \epsilon_0 - a$ and $\epsilon_0 = 78.4$ (dielectric constant in water in 25 C), $a = -8.5525$, $k = 7.7839$, and $\lambda = 0.003627 \text{ \AA}^{-1}$. The last term in Eq. 2 represents desolvation energy. In this work we used partial atomic volumes V and solvation coefficients S from Stouten et al.²⁶ In other words, the last term describes to what extent the protein buries the ligand in its interior.²⁷

3. Selection mechanism depends on scores of the ligand conformations. The lower effective interaction energy of a ligand, the higher the probability of surviving to a next epoch. We used the roulette selection scheme:

$$p_i = \frac{f^{(i)}}{\sum_{j=1}^n f^{(j)}}, \quad (4)$$

where $f^{(i)}$ is the score of the i th conformation, and p_i is the resulting probability of being selected to the next epoch.

4. Randomly selected ligand conformations undergo perturbations: combination and a Cauchy deviation. Conformations created during combination replace their precursors in the sampling set. The Cauchy deviation is performed by deviating the center of mass position by a number sampled from a Cauchy distribution.
5. Additional optimization procedure is applied in MAs, namely, a local search that leads to a faster convergence during the learning phase. We used two stochastic local searches: stochastic hill climbing (SHC),^{28,29} and the Solis-Wets method (SW).³⁰ In SHC the current ligand conformation is replaced only if a stochastically perturbed neighboring ligand has lower effective interaction energy. For this the algorithm proposed by Forest and Mitchell was used.²⁸ In the case of ligand-protein complexes, a random neighbor is created by the Cauchy deviation of the current ligand. In SW, the sampling domain is dynamically adjusted to increase the success rate of finding a better solution.^{24,25,31}
6. The steps described in 2–5 comprise an epoch. After multiple epochs the convergence is reached, and the ligand conformation with lowest effective interaction energy is taken as a next milestone. In other words, the unbinding proceeds in the direction of the selected conformation during the MD simulation. After a predefined number of steps the optimization procedure is repeated starting from the next ligand conformation.

We tested three variants of MAs: MA with SHC (MA-SHC), MA with SW (MA-SW), and MA without a local search employed (MA).

III. SIMULATION PROTOCOL

A. Optimization Parameters

In the test systems studied with MAs, the size of the learning set was 20. Ligand conformations were deviated by perturbing their center of mass positions. This was applied to a randomly chosen conformation with the probability of 0.02. The mean and spread of Cauchy distribution were set to 0 and 1, respectively. The optimization process was stopped after 20 epochs. The combination rate was set to 0.8. The local searches were applied to a randomly selected conformation with the probability of 0.67. The sampling radius, r_s from which conformations were sampled was 8 Å in M2-QNB, 15 Å in NHase-NCA, and 10 Å P450cam-camphor.

For the parameters used in the mRAMD simulations see Tabs. I-III, and for details regarding the MA simulations of the ligand-protein complexes, see Supporting Material.

B. Implementation

The main advantage of our program is a capability to compute ligand unbinding pathways during MD simulations. We used NAMD2.9 code³² to perform MD simulations with the CHARMM27 force field.³³ The communication between NAMD and the implemented program is done via NAMD’s feature called external program forces which is an interface to calculate biasing forces. The methods presented in this study were implemented in the C++11 programming language³⁴ using boost.³⁵ The code is available on Github (<https://github.com/jakryd/maze-namd>).

IV. RESULTS AND DISCUSSION

We studied ligand unbinding paths in the following model systems: M2 muscarinic receptor, nitrile hydratase, and cytochrome P450cam. In these complexes the channels accessible to ligands show increasing complexity (Fig. 1). We used mRAMD and MAs to sample ligand unbinding pathways and compared the results with RAMD. The resulting unbinding paths of are schematically presented in Fig. 2. In order to assess the efficiency of methods, a simple statistics was collected for each model system, for instance, the success rate of dissociation, defined as a ratio of the number of successful ligand exits from the protein tunnel to the number of all computational trials for a given method.^{17,36} We note that unbinding times in simulations are short because unbinding forces used to enforce dissociation events for each complex were high.

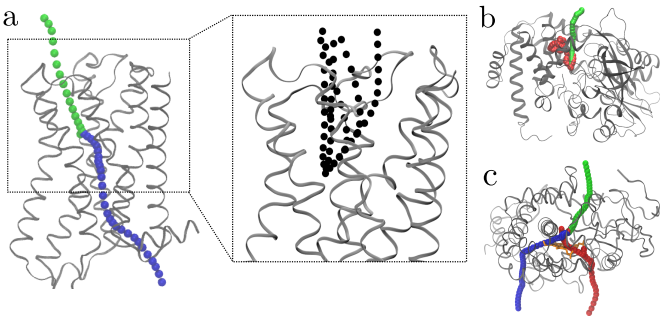


FIG. 2. Example ligand unbinding reaction pathways of the studied receptors. (a) M2-QNB complex: PW1 (green), PW2 (blue); example trajectories of PW1 (black) are given in the inset, (b) NHase-nicotinamide complex: PW (green), a trajectory that did not dissociate during a RAMD simulation (red), (c) P450cam-camphor complex: PW1 (blue), PW2 (green), PWC (red).

A. QNB in the M2 Muscarinic Receptor

In M2, the antagonist is buried 20 Å inside a regular cylindrical cavity (Fig. 1). We found two QNB dissociation pathways. The shapes of the PW1 egress trajectories (Fig. 2) are similar in all the methods studied, which perhaps means that it is a natural way for QNB to reach the exterior of M2. However, the average distance of diffusion, as indicated by the parameter Avg. d in Tab. I, is the shortest for the path predicted by mRAMD and MA (25 Å). For RAMD the ligand had to travel approximately 30 Å before reaching the receptor exterior region. The M2 muscarinic receptor with the QNB ligand bound is in an inactive conformation which means that a hydrophobic gate consisting of 3 amino acids (LEU65, LEU114, ILE392) is tightly closed.³⁷ There are also theoretical studies showing that such a hydrophobic gate is connected with an activation of G-protein-coupled receptors.³⁸ In M2, the hydrophobic gate is lying approximately 3 Å below the binding pocket of M2 and it blocks the PW2 egress pathways. The closed hydrophobic gate lowers the probability of sampling PW2 in our calculations. To confirm this hypothesis, we run multiple SMD simulations in the directions of exits identified by PW1 and PW2. The pulling forces needed to rupture

TABLE I. Characteristics of the unbinding pathways in the M2-QNB complex. The results of the simulations for the force constant $-f$ [kcal/mol Å], m – the frequency of choosing the next unbinding direction (in steps), N – the number of simulations, N_p – the number of successful unbinding trajectories for a given pathway. Values for unbinding time t [ps], work w [kcal/mol], and distance d [Å] are shown.

Method	Pathway	f	m	N	N_p	Min. t	Avg. t	Max. t	Min. d	Avg. d	Max. d	Min. w	Avg. w	Max. w
RAMD	PW1	5	10	20	9	0.86	1.11	1.35	26.56	30.15	37.30	75.6	100.4	126.3
RAMD	PW2	5	10	20	3	0.77	1.57	2.34	15.92	43.86	64.14	78.3	118.7	179.9
RAMD	PW1	10	10	20	5	0.45	0.72	0.99	24.84	38.39	65.73	193.0	260.4	408.5
RAMD	PW2	10	10	20	6	0.98	1.24	1.44	43.84	60.57	79.80	326.2	442.6	595.9
mRAMD	PW1	5	10	9	6	0.75	1.11	1.65	21.15	29.16	36.59	71.7	93.9	115.6
mRAMD-LES	PW1	5	10	10	10	0.64	0.9	1.14	18.18	25.49	32.77	63.7	89.7	118.7
MA	PW1	5	50	20	12	0.55	0.71	0.97	18.26	24.47	31.94	70.8	111.4	148.5
MA-SHC	PW1	5	50	10	9	0.51	0.79	1.18	17.39	26.58	39.08	83.4	117.6	182.9
MA-SW	PW1	5	30	10	8	0.57	0.85	1.25	17.76	28.57	41.02	80.0	126.1	164.4

the hydrophobic gate through PW2 were higher by approximately 300 pN, comparing to the highest force resulted on PW1. Moreover, in a recent paper by Kruse et al.³⁹ authors studied QNB diffusion paths in the M3 muscarinic receptor which has a similar GPCR structure. Numerous very long MD simulations (nearly 25 microseconds) were used to estimate pathways for the spontaneous QNB association with the M3 receptor. The paths found in that paper are qualitatively similar to PW1 which suggests that PW1 is preferable for QNB.

We compared work done by unbinding force in the tested methods. It is the lowest in MAs, and has a value of about 90 kcal/mol, while the lowest value for Avg. w in RAMD is 100 kcal/mol. Thus, we expect that the perturbations of the receptor structure induced by the process of ligand dissociation are smaller in mRAMD and MAs than it is in RAMD, which is another advantage of the proposed methods (Fig. 3). It is worth noting that Avg. w for PW2 trajectories calculated by RAMD was as high as 442 kcal/mol (Tab. I).

B. Non-Convex Optimization Performs better for Curved Nitrile Hydratase Tunnel

We calculated ligand exit paths for the nicotinamide-NHase system starting from the ligand buried approximately 40 Å beneath the protein surface. In contrast to the M2 receptor the channel is curved, thus diffusion in this case is more challenging from the methodological point of view. The methods found the same exit pathway, PW (Fig. 2b). It is in a good agreement with our previous LES calculations for other amides.⁴⁰ The results of the success rate and pathway characteristics are presented in Tab. II. mRAMD shows a moderate success rate for this system, 44%. However, when information on possible ligand conformations is obtained from LES, the success rate rises up to 90% (Tab. II). Clearly this suggests that LES performs better the initial sampling of the protein interior due to lowered potential energy barriers.

MAs show an excellent success rate, despite the lack of the initial sampling: MA - 90% , MA-SHC - 100%, and MA-SW - 100%. The success rate of RAMD is low: 0%-14%. If the unbinding path is found, the mean unbinding time Avg. t in RAMD is 5 times higher than in mRAMD. It shows that the algorithms with a more advanced sampling scheme find optimal egress pathways. The lowest value for the work performed during ligand unbinding is about 69 kcal/mol for MA-SW, and the largest value of 482 kcal/mol resulted from RAMD.

C. Sampling Transient Tunnels in Cytochrome P450cam

As the last and the most complex test case, cytochrome P450cam from *Pseudomonas Putida* was used (Fig. 1). During the P450cam activity camphor enters a distal pocket buried inside the enzyme and located close to the heme moiety. As previously said, Lüdemann et al. used RAMD to study possible camphor dissociation paths.¹¹ After

TABLE II. Characteristics of the unbinding pathways in the NHase-NCA complex. The results of the simulations for the force constant $-f$ [kcal/mol Å], m – the frequency of choosing the next unbinding direction (in steps), N - the number of simulations, N_p - the number of successful unbinding trajectories for a given pathway. Values for unbinding time t [ps], work w [kcal/mol], and distance d [Å] are shown.

Method	Pathway	f	m	N	N_p	Min. t	Avg. t	Max. t	Min. d	Avg. d	Max. d	Min. w	Avg. w	Max. w
RAMD	PW	10	50	14	2	5.35	5.75	6.15	49.72	117.48	185.24	247.9	482.0	716.1
RAMD	PW	15	30	7	0	—	—	—	—	—	—	—	—	—
mRAMD	PW	10	100	9	4	1.15	3.71	6.00	38.96	77.64	153.78	121.9	242.1	473.3
mRAMD-LES	PW	10	100	10	9	1.15	1.61	1.95	33.85	42.66	55.03	82.1	106.5	134.7
MA	PW	10	50	10	9	1.30	1.68	1.90	31.45	46.83	54.41	49.5	76.5	95.6
MA-SHC	PW	10	50	15	15	1.10	1.66	1.95	21.07	44.49	54.56	36.7	72.5	89.0
MA-SW	PW	10	50	10	10	1.55	1.63	1.80	32.57	43.33	49.18	44.0	69.5	77.4

running hundreds of simulations the authors found three distinct routes (1, 2, 3), but for the path no. 2 three variants were observed. The results of our RAMD calculations for P450cam agree with those obtained by Lüdemann et al. we found three groups of pathways as well. PW1 path (Fig. 2c) is identical to that presented in Lüdemann et al. The same refers to our PW2 and the pathway no. 2a. However, we were not able to observe path no. 3. Instead we found the third pathway in P450cam, which corresponds to so-called water channel (PWC, Fig. 2c). PWC corresponds to a hydrophilic channel located near the heme propionic groups, and was already suggested as the exit channel for the product, 5-hydroxy-camphor, which is more hydrophilic than camphor.^{41,42} There are lacking evidences that show the existence of PWC in P450s cytochromes in standard RAMD calculations.^{43–45} The function of PWC is not clear so far. It may have a role in the passage of water and molecular oxygen. PWC opens towards the proximal side of the heme group, which suggests, that it may have a role in the electron transport system.⁴⁵ Alternatively, it may be involved in the transport of protons through a network of ordered water molecules.⁴⁶

The detailed results on the pathways in cytochrome P450cam are presented in Tab. III. One can see that only 60% of the RAMD trials led to camphor exit ($f = 10$ kcal/molÅ). If the force constant of $f = 5$ kcal/molÅ was used in RAMD, the success rate was even lower (20%). However, in the case of MAs proposed here, the success rates were much better. mRAMD gave the 80% success rate, and mRAMD with LES provided 100% (PW1 30%, PW2 70%). All the variants of MA-based methods gave a 100% success rate. The majority of the methods predicts that PW2 dominates in the camphor transport in cytochrome P450cam, in accordance with the earlier report.¹¹

mRAMD needs 2.63 ps to find an exit for the same conditions as for RAMD (PW2, $f = 5$ kcal/molÅ), thus the total simulation time for mRAMD is approximately 3 times shorter than in RAMD. A comparison of the distance traveled by camphor in both cases (Avg. d , Tab. III) favors mRAMD as well (43.8 Å and 25.53 Å for RAMD and mRAMD, respectively). Interestingly, the shortest distance path PW2 was predicted by the MA-SW method (15.44 Å). This very short path was quickly found (Avg. t , 1.53 ps) due to a variable sampling domain adopted in the IA-SW algorithm. This feature is particularly advantageous when the diffusion channel is very narrow, like in P450cam. All the other methods needed numerous trials before a successful unbinding direction was determined. Here, in MA-SW a larger sampling domains quickly brings information that larger area is available for a ligand. The work Avg. w (see Tab. III) performed by unbinding force along PW2 is the smallest one (66 kcal/mol). A relatively low work of 90 kcal/mol is needed to force camphor through PW2 as predicted by mRAMD, but as much as 305 kcal/mol is required to run the ligand along PW1 by RAMD.

D. Summary

The summary of the success rates for all algorithms is presented in Tab. IV. We calculated the ratio of a number of successful paths to the number of all exit simulation attempts. The results show that the best average success rate (Avg. SR) of 96.7% is offered by the MERA-LES algorithm, but one needs to remember that the mRAMD-LES

TABLE III. Characteristics of the unbinding pathways in the P450cam-CAM complex. The results of the simulations for the force constant $-f$ [kcal/mol Å], m – the frequency of choosing the next unbinding direction (in steps), N – the number of simulations, N_p – the number of successful unbinding trajectories for a given pathway. Values for unbinding time t [ps], work w [kcal/mol], and distance d [Å] are shown.

Algorithm	Pathway	f	m	N	N_p	Min. t	Avg. t	Max. t	Min. d	Avg. d	Max. d	Min. w	Avg. w	Max. w
RAMD	PW1	10	100	10	2	1.30	2.03	2.75	33.06	49.83	66.60	287.6	417.6	270.4
RAMD	PW2	10	100	10	3	1.05	1.15	1.30	27.73	29.16	30.67	214.4	242.8	270.4
RAMD	PWC	10	100	10	1	2.05	2.05	2.05	39.96	39.96	39.96	305.2	305.2	305.2
RAMD	PW2	5	100	10	2	2.10	7.30	12.5	25.83	43.88	61.92	114.1	178.3	242.5
mRAMD	PW1	5	100	10	3	2.10	2.63	2.90	25.59	31.26	39.12	85.4	106.7	141.8
mRAMD	PW2	5	100	10	5	1.00	1.87	2.85	18.16	25.53	34.55	68.1	92.8	130.1
mRAMD-LES	PW1	5	100	10	3	2.50	3.88	5.35	29.20	38.15	49.86	90.2	115.6	150.6
mRAMD-LES	PW2	5	100	10	7	3.30	3.90	4.30	28.96	36.82	48.09	72.9	119.5	156.7
MA	PW1	5	100	10	2	1.70	2.65	3.60	24.65	32.50	40.34	109.9	130.3	150.8
MA	PW2	5	100	10	8	1.00	1.61	2.60	20.59	24.25	36.89	92.8	109.8	152.6
MA-SHC	PW1	5	100	10	1	3.10	3.10	3.10	47.95	47.95	47.95	187.9	187.9	187.9
MA-SHC	PW2	5	100	10	6	1.45	2.90	4.30	22.00	43.84	55.51	97.5	174.9	215.6
MA-SHC	PWC	5	100	10	3	3.45	4.68	5.30	50.73	66.43	77.64	190.9	254.7	296.8
MA-SW	PW1	5	100	10	1	2.10	2.10	2.10	25.72	25.72	25.72	117.1	117.1	117.1
MA-SW	PW2	5	100	10	3	1.20	1.53	1.70	8.95	15.44	20.98	32.0	66.2	90.8
MA-SW	PWC	5	100	10	6	2.20	2.89	3.40	21.53	24.18	27.64	92.1	99.3	116.1

TABLE IV. Summary of the success rates for the ligand-protein complexes studied.

method	success rate			
	M2	NHase	P450cam	Avg.
RAMD	60	14	60	44.6
mRAMD	66	44	80	63.3
mRAMD-LES	100	90	100	96.7
MA	60	90	100	83.3
MA-SHC	90	100	100	96.7
MA-SW	80	100	100	93.3

calculations were based on the pre-calculated ligand conformations by LES. Since MAs do not require similar pre-calculations, they are in some sense the most successful in our study. The MA-SHC and MA-SW methods display successful rate of 96.7% and 93.3%, respectively. The mRAMD algorithm has SR of 63.3% which is much better than RAMD (44.3%). Moreover, the new algorithms presented here show that collision statistics and the RMSD values generated during 10 randomly chosen trajectories for each system tested, are lower in MA, comparing to RAMD (FIG. 4, TABLE V). It is worth noting that despite the high percentage of successful dissociations, MA and mRAMD do not introduce excessive artifacts during the sampling of protein conformations.

V. CONCLUSIONS

Molecular modeling in biology, biophysics or drug design often requires computation of unbinding pathways within macromolecular matrices. The classical MD simulations can contribute to prediction of such processes, however, simulations of diffusion may be extremely time-consuming.

In this paper we have presented two types of new methods that alleviate these problems and improve the search for ligand unbinding pathways substantially: mRAMD and MAs. These methods have been tested on three protein-ligand systems with increasing complexity of the channels: M2 muscarinic receptor and QNB, nitrile hydratase and

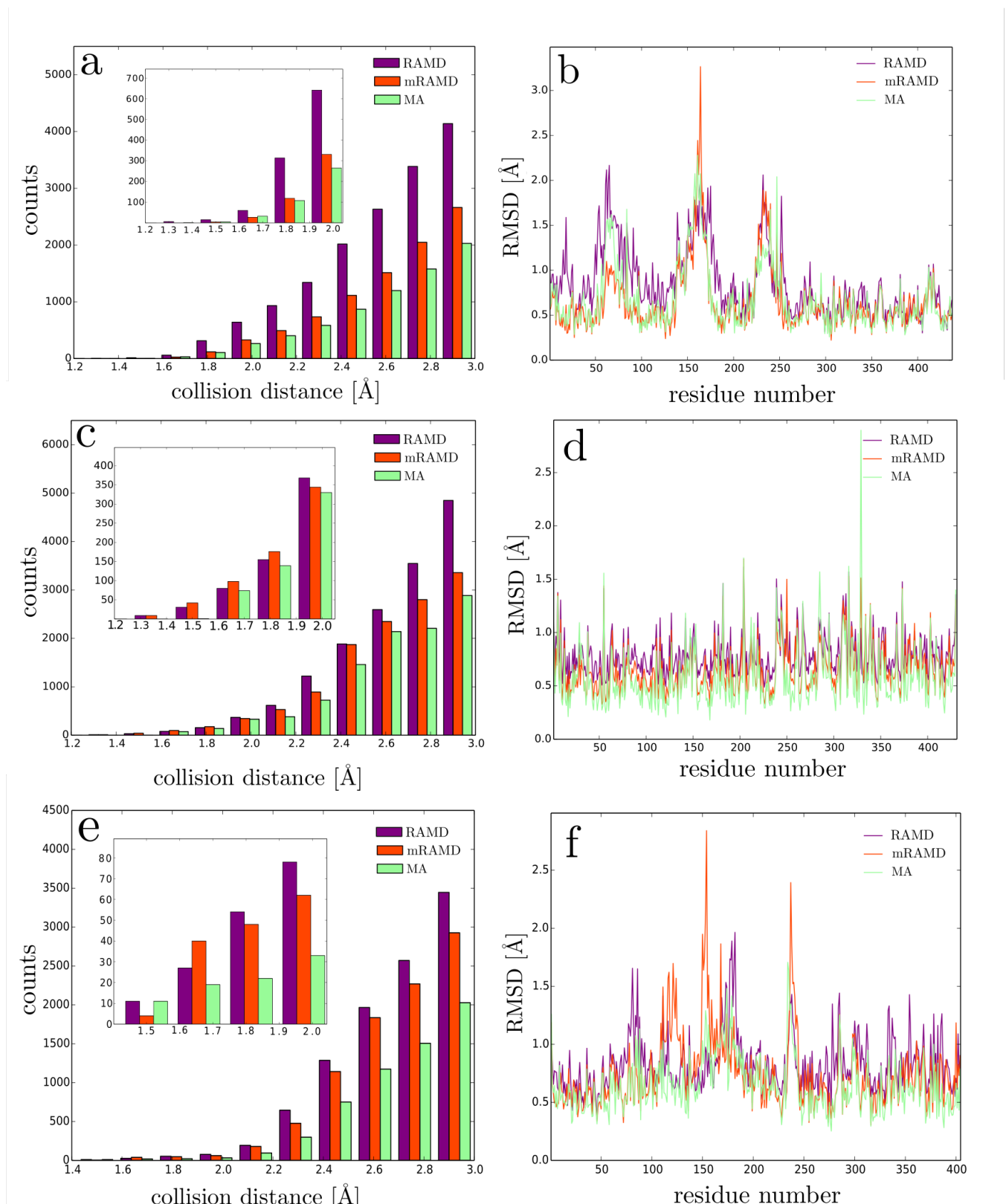


FIG. 3. Average RMSD per residue (b, d, f) and the collision statistics (a, c, e) of the M2-QNB (a, b), NHase-nicotinamide (c, d) and P450cam-camphor (e, f) complexes from 10 randomly chosen trajectories. Insets (a, c, e) depict zoomed histograms for the collision distance < 2 Å.

nicotinamide, and cytochrome P450 and camphor.

In mRAMD, a memory was added to RAMD. Calculations showed that this method may improve RAMD. Moreover, in our variant we used locally enhanced sampling⁵ to calculate initial distribution of ligand conformations within the protein matrices. The resulting method showed a high success rate (96%). One should note that LES pre-calculations require additional, but reasonable computing time.

The other group of new methods is based on optimization. In MAs a scoring function based on ligand-protein effective interaction energy is used to assess the unbinding direction. We showed that local searches may be a good solution for further optimization. The success rate of MAs is 93-96% and they do not require any pre-calculations, as opposed to mRAMD.

ACKNOWLEDGMENTS

This research was supported in part (WN) by the NCN grant N N202 262038. We thank for computer time allocated in the Interdisciplinary Center for Modern Technologies, NCU. We would like to thank Rafal Jakubowski for useful discussions, and Aleksander Balter and Magdalena Ryzewska for reading over the manuscript.

- ¹J. Ryzewski and W. Nowak, *J. Chem. Phys.* **143**, 124101 (2016).
- ²U. S. Bhalla and R. Iyengar, *Science* **283**, 381 (1999).
- ³P. J. Tummino and R. A. Copeland, *Biochemistry* **47**, 5481 (2008).
- ⁴M. Bhat, *Biotechnol. Adv.* **18**, 355 (2000).
- ⁵R. Elber and M. Karplus, *J. Am. Chem. Soc.* **112**, 9161 (1990).
- ⁶W. Nowak, R. Czerminski, and R. Elber, *J. Am. Chem. Soc.* **113**, 5627 (1991).
- ⁷J. Schlitter, M. Engels, and P. Krüger, *J. Mol. Graphics* **12**, 84 (1994).
- ⁸D. Kosztin, S. Izrailev, and K. Schulten, *Biophys. J.* **76**, 188 (1999).
- ⁹D. Sabbadin and S. Moro, *J. Chem. Inf. Model.* **54**, 372 (2014).
- ¹⁰J. M. Johnston and M. Filizola, in *G Protein-Coupled Receptors-Modeling and Simulation* (Springer, 2014) pp. 95–125.
- ¹¹S. K. Lüdemann, V. Lounnas, and R. C. Wade, *J. Mol. Biol.* **303**, 797 (2000).
- ¹²T. Wang and Y. Duan, *J. Am. Chem. Soc.* **129**, 6970 (2007).
- ¹³T. Wang and Y. Duan, *J. Mol. Biol.* **392**, 1102 (2009).
- ¹⁴M. Klvana, M. Pavlova, T. Koudelakova, R. Chaloupkova, P. Dvorak, Z. Prokop, A. Stsiapanava, M. Kutý, I. Kuta-Smatanova, J. Dohnalek, *et al.*, *J. Mol. Biol.* **392**, 1339 (2009).
- ¹⁵W. Li, J. Shen, G. Liu, Y. Tang, and T. Hoshino, *Proteins* **79**, 271 (2011).
- ¹⁶S. Kalyaanamoorthy and Y.-P. P. Chen, *J. Chem. Inf. Model.* **52**, 589 (2012).
- ¹⁷H. Vashisth and C. F. Abrams, *Biophys. J.* **95**, 4193 (2008).
- ¹⁸M. Dorigo and T. Stützle, in *Handbook of Metaheuristics* (Springer, 2003) pp. 250–285.
- ¹⁹D. Shepard, in *Proceedings of the 1968 23rd ACM national conference* (ACM, 1968) pp. 517–524.
- ²⁰J. H. Friedman, J. L. Bentley, and R. A. Finkel, *ACM Transactions on Mathematical Software (TOMS)* **3**, 209 (1977).
- ²¹T. Liszka, *Int. J. Numer. Meth. Eng.* **20**, 1599 (1984).
- ²²D. E. Goldberg, *Genetic algorithms* (Pearson Education India, 2006).
- ²³Z. Michalewicz, *Genetic algorithms + data structures = evolution programs* (Springer, 1996).
- ²⁴G. M. Morris, D. S. Goodsell, R. S. Halliday, R. Huey, W. E. Hart, R. K. Belew, and A. J. Olson, *J. Comput. Chem.* **19**, 1639 (1998).
- ²⁵D. S. Goodsell and A. J. Olson, *Proteins* **8**, 195 (1990).
- ²⁶P. F. Stouten, C. Frömmel, H. Nakamura, and C. Sander, *Mol. Simulat.* **10**, 97 (1993).
- ²⁷L. Wesson and D. Eisenberg, *Protein Sci.* **1**, 227 (1992).
- ²⁸M. Mitchell, J. H. Holland, and S. Forrest, in *NIPS* (1993) pp. 51–58.
- ²⁹D. B. Skalak, in *ICML* (Citeseer, 1994) pp. 293–301.
- ³⁰F. J. Solis and R. J.-B. Wets, *Math. Oper. Res.* **6**, 19 (1981).
- ³¹W. E. Hart, *Adaptive Global Optimization with Local Search*, Ph.D. thesis, University of California, San Diego (1994).
- ³²J. C. Phillips, R. Braun, W. Wang, J. Gumbart, E. Tajkhorshid, E. Villa, C. Chipot, R. D. Skeel, L. Kale, and K. Schulten, *J. Comput. Chem.* **26**, 1781 (2005).
- ³³B. R. Brooks, R. E. Bruccoleri, B. D. Olafson, D. J. States, S. Swaminathan, and M. Karplus, *J. Comput. Chem.* **4**, 187 (1983).
- ³⁴B. Stroustrup, *The C++ programming language* (Pearson Education India, 1995).
- ³⁵B. Karlsson, *Beyond the C++ standard library: an introduction to boost* (Pearson Education, 2005).
- ³⁶P. Carlsson, S. Burendahl, and L. Nilsson, *Biophys. J.* **91**, 3151 (2006).

- ³⁷K. Haga, A. C. Kruse, H. Asada, T. Yurugi-Kobayashi, M. Shiroishi, C. Zhang, W. I. Weis, T. Okada, B. K. Kobilka, and T. Haga, *Nature* **482**, 547 (2012).
- ³⁸S. Yuan, S. Filipek, K. Palczewski, and H. Vogel, *Nat. Commun.* **5** (2014).
- ³⁹A. C. Kruse, J. Hu, A. C. Pan, D. H. Arlow, D. M. Rosenbaum, E. Rosemond, H. F. Green, T. Liu, P. S. Chae, and R. O. Dror, *Nature* **482**, 552 (2012).
- ⁴⁰L. Peplowski, K. Kubiak, and W. Nowak, *Chem. Phys. Lett.* **467**, 144 (2008).
- ⁴¹T. L. Poulos, B. C. Finzel, and A. J. Howard, *Biochemistry* **25**, 5314 (1986).
- ⁴²T. I. Oprea, G. Hummer, and A. E. García, *Proc. Natl. Acad. Sci. U.S.A.* **94**, 2133 (1997).
- ⁴³K. Schleinkofer, P. J. Winn, S. K. Lüdemann, R. C. Wade, *et al.*, *EMBO Rep.* **6**, 584 (2005).
- ⁴⁴P. J. Winn, S. K. Lüdemann, R. Gauges, V. Lounnas, and R. C. Wade, *Proc. Natl. Acad. Sci. U.S.A.* **99**, 5361 (2002).
- ⁴⁵R. C. Wade, P. J. Winn, I. Schlichting, *et al.*, *J. Inorg. Biochem.* **98**, 1175 (2004).
- ⁴⁶S. Vohra, M. Musgaard, S. G. Bell, L.-L. Wong, W. Zhou, and P. C. Biggin, *Protein Sci.* **22**, 1218 (2013).